

# **Successful Application of Ground Penetrating Radar in the Exploration of Gem Tourmaline Pegmatites of Southern California**

**Jeffrey E. Patterson and Frederick A. Cook**

Department of Geology and Geophysics

**University of Calgary**

Calgary, AB T2N 1N4 Canada

## **Abstract**

Application of ground penetrating radar has been successful in delineating gem-bearing zones in the Himalaya pegmatite mine of the Mesa Grande district of southern California. The high frequency of the electromagnetic signal allows features as small as a few cm to be resolved within 1-2 meters of the surface of a mine wall. Careful initial setup consisted of: 1) selection of antennas with sufficiently high central frequencies, 2) recording with a short time of scan to reduce end of scan noise levels, and 3) choosing appropriate color schemes to highlight extreme amplitude variations. Operation during data collection insisted of pre-painting marking points on the mine face and air launching the signal to reduce false anomalies caused by rocking of the antenna on the rough surfaces. Data processing using the Hilbert Transform provided images of the cavity geometry that was then used by the blasting captain for accurate placement of explosives. The instantaneous frequency plot was found to be effective for distinguishing air from clay filled pockets, and the instantaneous phase plot was helpful in selecting potential targets where the amplitude was less than the maximum range. When carefully used in conjunction with good knowledge of the geological conditions, the method promises to provide an important tool for mapping internal structures of pegmatites and thus assisting future mining activities.

## **Introduction**

The use of ground penetrating radar (GPR) in engineering, archaeology, and surficial environmental geology studies is well documented and highly effective, (Ulrickson, 1982, Pilon, ed., 1992, Conyers and Goodman, 1997, Arcone, 1998, Noon, et.al., 2000). However, applications of the technique in crystalline rocks have been primarily devoted to delineating cracks for engineering applications or nuclear waste storage facilities (Grasmueck, 1996, Tillard, 1996, Holloway, 1992; Olson, et.al., 1992). Direct application in hardrock mining has been conducted for the past 30 years, but scientific publication of this effort is limited and generally details use of borehole radar information, (Cook, 1973, Dolphin, et.al., 1978, GSSI, 2000, Franké and Nobes, 2000, Trickett, et.al., 2000). Identification of mineralized zones, in granitic rocks for example, has been somewhat elusive (Lees, 1998). Although the resolution that is possible with high frequency (500 MHz to 1 GHz) radar signals is not generally necessary for exploration of large mineral deposits such as base metals, it may potentially provide a practical method of identifying small (to a few cm), but economically viable, gem bearing cavities (vugs and pockets) in granitic pegmatites.

Each of us independently hypothesized in 1995 that GPR could be an appropriate tool for gemstone exploration in the near surface, as well as in subsurface exposures in adits, drifts and stopes of many gem mines (Patterson, 1996; Cook, 1997). As a result of a review in 1996 of Cook (1997), by

the late Eugene E. Foord of the USGS, we became aware of each other's work. For nearly 5 years since, we have been applying a variety of GPR instruments, parameters, and data processing methods in pegmatite mines of southern California (Figure 1) in an effort to establish optimum parameters for imaging miarolitic gem-bearing cavities (pockets and vugs). The culmination of these efforts was reached during our work in the Himalaya mine pegmatite of the Mesa Grande district in June, 1998, with the first documented discovery of gem tourmaline pockets and vugs using this technique (Patterson and Cook, 1999).

### Southern California Pegmatite Mines Investigated with Ground Penetrating Radar

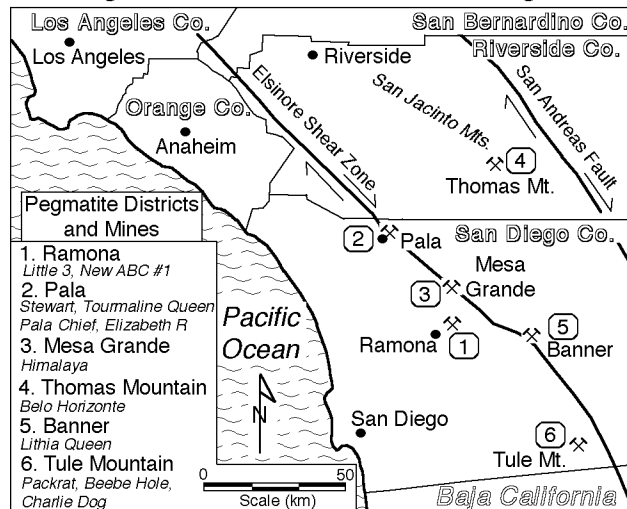


Figure 1. Location map of gem-bearing pegmatites in southern California at which we have applied ground penetrating radar since 1995. These are numbered in chronological order of our work.

### Southern California Pegmatites

Successful interpretation of geophysical data requires good geological knowledge. Since 1995, we have undertaken a series of experimental programs to develop an understanding of granitic pegmatite systems and the responses of GPR (Ground Penetrating Radar) signals in these rocks. During this period, we have investigated the major gem-bearing pegmatite mines in southern California (Figure 1). The majority of the test work was undertaken at the Little 3 Mine near Ramona (Figure 1), where several sets of instruments were compared in a standard set of dike sections to determine operating characteristics and optimum recording parameters. The systems used included Geophysical Survey Systems, Inc. (GSSI) SIR II and SIR 3 GPRs with 100, 300, 500, 900, and 1,000 MHz antennas and Sensors & Software Pulse Echo IV GPR with a 200 MHz antenna and the PE 1000 GPR with a 450 MHz antenna. During this field activity, non-gem bearing vugs, dike contacts, and water or clay filled fractures were identified and their GPR responses catalogued.

Once these initial efforts were completed, we undertook reconnaissance studies at mines elsewhere in southern California. In 1997, during a survey at the Tourmaline Queen mine in Pala, an

anomalous zone was identified by us, subsequently excavated by the mine owner, and found to contain at least two 3 cm by 10 cm gem Indicolite tourmaline crystals. Although the find was not measured and calibrated against the recorded radar signal for scientific verification, we were able to observe the geological characteristics of the excavated zone and compare this with the scanned signal for future reference. Later in 1997, at the Lithia Queen mine in Banner (Figure 1), we identified and excavated an air filled cavity and fracture system at 1.25 m depth, but no gem crystals were found. Both of these surveys used a Sensors & Software PE 1000 GPR with a 450 MHz central frequency antenna.

The tabular granitic pegmatites of southern California (Figure 1) have produced gem tourmaline and other rare minerals for more than 130 years. The pegmatites are found in a number of localized regions (districts) from Riverside County into Baja California, a distance of about 250-300 km, generally along the Elsinore (and associated) shear zones (Figure 1). Although mineralogy varies somewhat from one district to another, and even from dike to dike within a district, the dikes were all intruded into the late Cretaceous (120 ma to 105 ma) Peninsular Ranges batholith gabbroic to granodioritic and related rocks between about 106 ma and 85ma, (Silver, et.al., 1979; Krummenacher, et al., 1975). The dikes typically strike north to northwest and dip west to west-southwest between 20° and 40°. Tabular gem bearing pegmatites are found throughout in the world in similar tectonic settings, including Maine, Virginia, North Carolina, and Colorado, USA; Elba, Italy; Nuristan, Afghanistan; Stak Nala, Pakistan; Central Ural Mountains and Transbikalia District, Russia; Pamir Mountains, Tajikistan; O'Grady Batholith, NWT, Canada; Minas Gerais, Brazil; Madagascar; Nigeria; and Namibia. Thus, we consider that the results from the studies in southern California may have application elsewhere.

The Himalaya mine, located in the Mesa Grande district (Figure 1), has been the major southern California producer of gem elbaite tourmaline and other rare pegmatite minerals for the past 103 years. The pegmatites in this district form a series of tabular sub-parallel en-echelon dikes whose individual thickness rarely exceed one meter (Figure 2a). These dikes generally strike 340° to 010°, nominally dip 20°-35° southwest, and have exposure lengths of about 1.2 km (Donnelly, 1935). The dikes were intruded into the Cretaceous San Marcos gabbro-norite (Donnelly, 1935) at about 98 ma (Foord, 1976). Access to the Himalaya mine dike system is through a series of underground galleries, drifts, and stopes, thus affording over 6,000 m of dike exposure (Fisher, et.al., 1998).

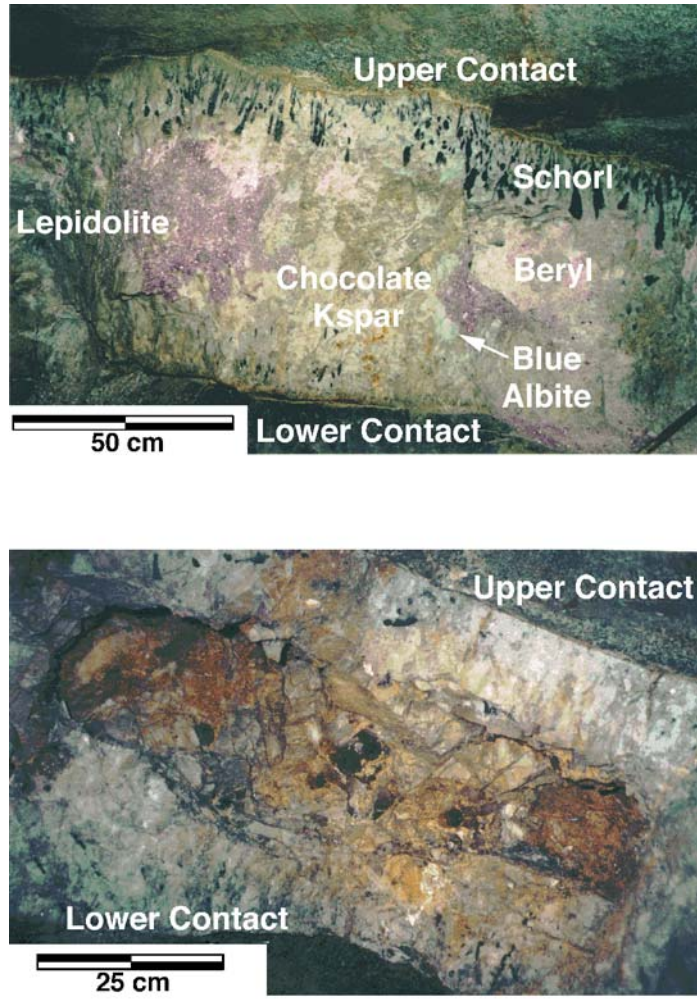


Figure 2. a) Photograph of a portion of Himalaya dike illustrating many features that are considered "typical" indications of gem-bearing pockets. These include: schorl crystals that flare toward the center of the dike and grade into elbaite, pods of lavender lepidolite, opaque morganite beryl, "chocolate" K-feldspar, and blue albite. (b) An excavated pocket that has the expected flattened shape near the center of the dike. Note that the pocket is approximately parallel to the dike contacts. This pocket was found with GPR (File 519) after the discovery at pocket 441. Note that quartz crystals and **clevelandite** feldspar masses are still attached near the center.

Mining activities in these pegmatites are often guided by the assumptions that most pockets are flattened, bladder like spaces parallel to the dike contacts (Figure 2b), and that specific mineralogical changes occur in the vicinity of pockets so that these characteristics can be used as indicators when mining activities approach a potentially productive zone (e.g., Donnelly, 1935). Such indicators include: 1) prominent schorl (black, sodium-iron rich tourmaline) crystals that flare towards the center of the dike and change in both color and composition along their c-axes to elbaite (multi-colored to pink, sodium-lithium-aluminum rich tourmaline), and, 2) pods of fine-grained lavender lepidolite (lithium and fluorine rich mica (Figure 2a). Although these are often valid characteristics, in many areas the signs are subtle, non-existent, or occur over such a short distance from a pocket (less than a few cm) that they can be easily missed (Figure 3a). The objectives of GPR is thus to provide a means

of identifying regions with potential for gem-bearing pockets or cavities in the absence of visible mineralogical indicators and to provide an easily interpretable image to guide the mining blasting captain in setting charges for excavating the pockets. Often, for example, pockets and their contents will be destroyed during mining operations due to a lack of precise knowledge of the pocket location.

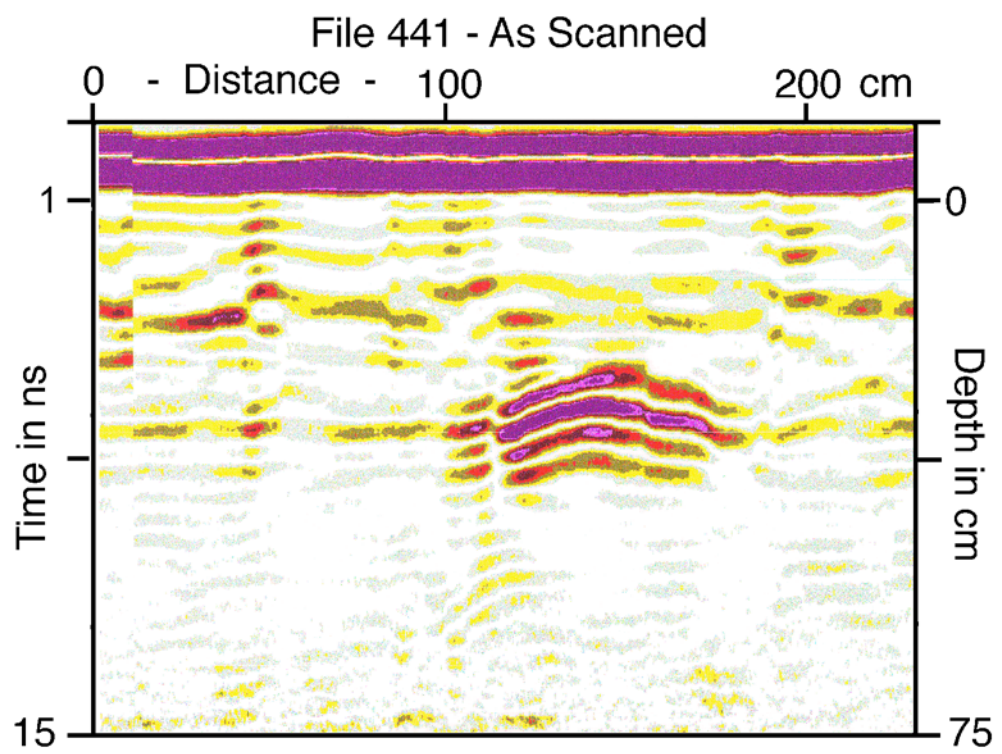
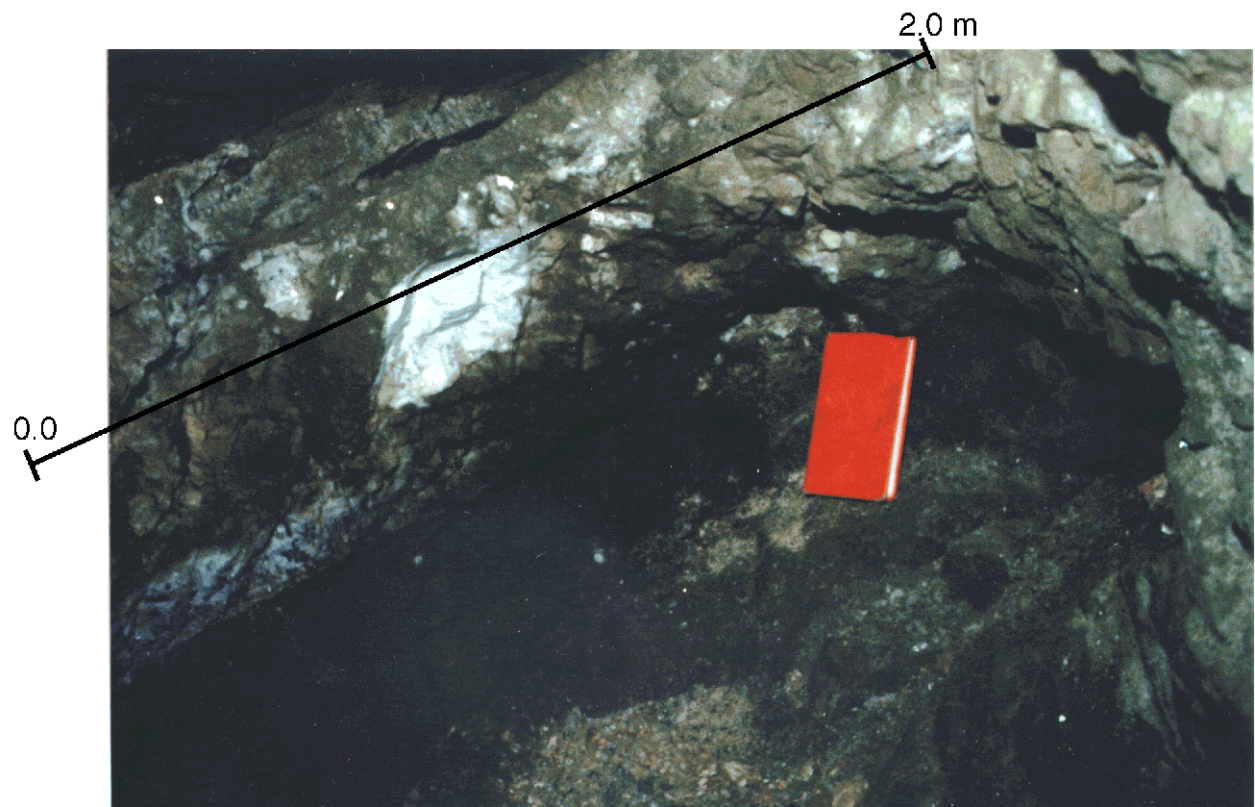
Several characteristics of these cavities and surrounding dike make it difficult to distinguish them. First, the cavities are not smooth sided; the interior surfaces are generally very rough, with crystals of quartz, tourmaline, clevelandite (sodium plagioclase), microcline, and lepidolite projecting inward. These rough surfaces tend to scatter and thus diminish the signals. Second, the majority of the pockets are filled with a mixture of dry to saturated saponite, montmorillonite, or kaolinite clays and occasionally zeolites. In most cases, the tourmaline and quartz crystals have been sheared from the walls and are suspended within the clay or zeolite fillings along with shards of feldspars and balls of lepidolite. Finally, nearby contact-to-contact fractures are also filled with saturated red clays that can give spurious signal returns.

## Methods

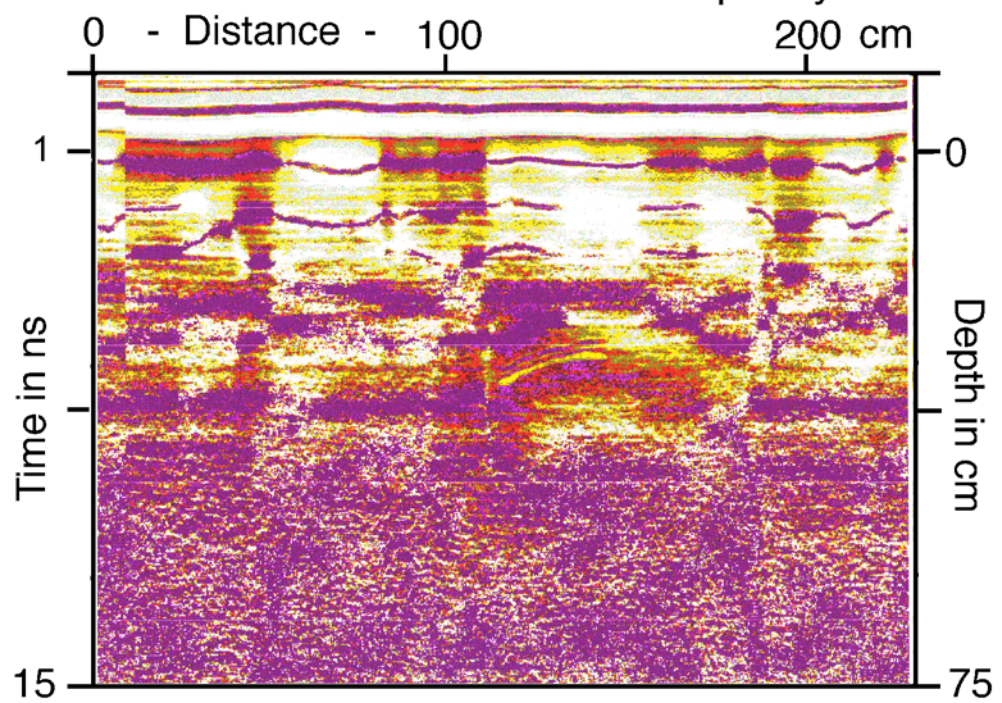
### Data Acquisition

In ground penetrating radar, an electromagnetic pulse of several nanoseconds duration ( $1 \text{ ns} = 1 \times 10^{-9} \text{ s}$ ) is transmitted via a tuned antenna into the subsurface where it may respond from rocks with contrasting electrical properties. Returned signals are sensed by a receiving antenna and recorded digitally in a manner similar to seismic prospecting. This allows the signals to be displayed, processed and enhanced using many standard signal-processing techniques. In most applications, the radar antennas are located on the earth's surface so that the signals penetrate vertically down and back. In our underground applications, however, the antennas were typically directed into the working face of the dike such that the resulting images represented signals penetrating into the dike and responding from internal contrasts or external contacts before being returned to the receiver. The data in these surveys were acquired using a GSSI SIR-II GPR with antennas ranging 500, 900, and 1,000 MHz central frequencies, for the underground work (Table 1).

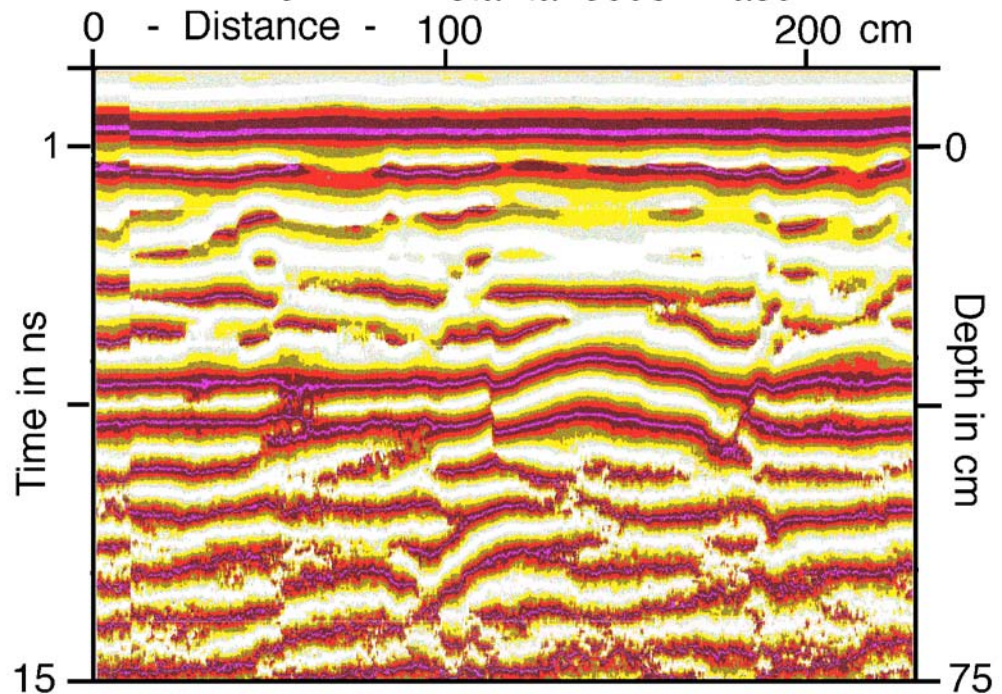
The data for illustrated here (Figures 3 and 4) were collected in June, 1998, using a GSSI, SIR-II, GPR with a 1,000 MHz central frequency antenna. Parameter selections to the scanning program were made via the fixed operating environment of the SIR-II. The method of scan was based on a continuous profile, in which the antenna was held approximately 10 cm away from the face of the dike, and then moved in-plane parallel to the inclination of the dike, about  $32^\circ$  updip for File 441 (Figures 3 & 6). Although this technique produces a prominent air wave (Figure 3b) it reduces the effects of irregularities on the surface of the dike that cause spurious signals as the antenna bumps along the surface. This approach also allowed the signal to be directed into the most productive region of the dike. Although there is some signal loss using this method, over the method whereby the antenna maintains direct contact with the rock face, the reduction in "false returns" provided far superior data (Wensink et.al., 1990; Glover, 1992).



File 441 - Instantaneous Frequency



File 441 - Instantaneous Phase



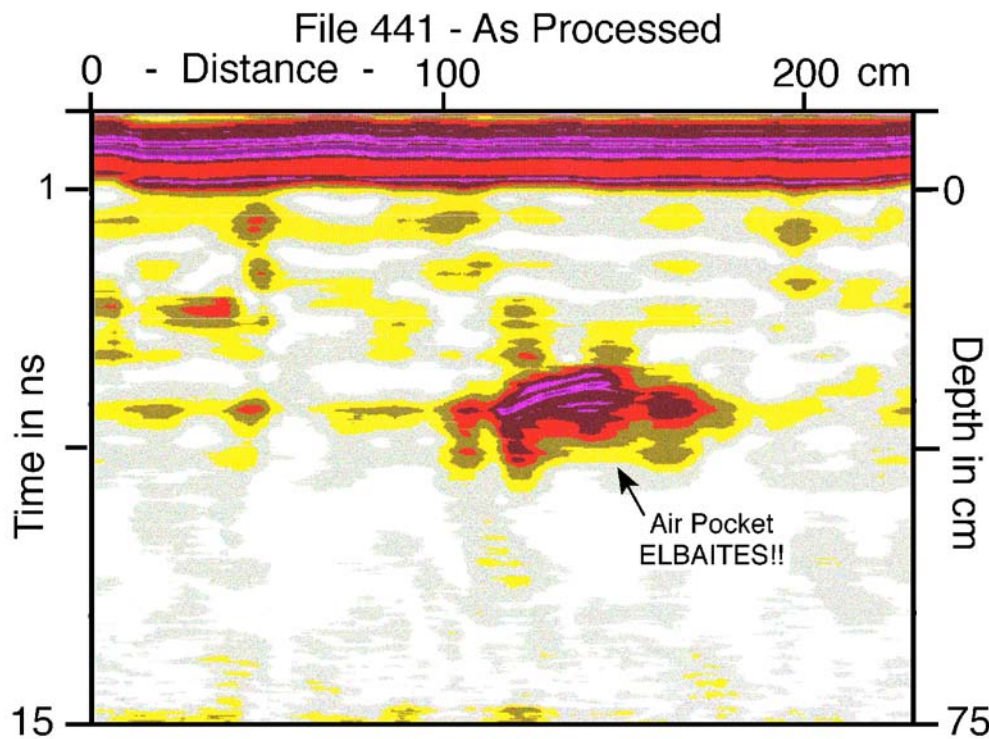


Figure 3. a) Section of dike along which the radar scan was run prior to cleaning and excavation. The dike is covered in blast dust and exhibits no obvious signs that would indicate pocket development. The line with 0.0-2.0m marks the line of traverse of the profile described here. b) Original scan (1,000 MHz) along the face of the dike illustrates a prominent anomaly centered near 1.5 m and 8 ns. Additional smaller anomalies are visible near 0.5 m, 8 ns and 0.5 m, 4 ns. c) Instantaneous frequency of the data in Figure 3b. Although radar signals are non-stationary, frequency variations can indicate changes in dielectric properties; here the yellow line delineates a sharp edge of the anomaly thus suggesting a cavity wall. d) Instantaneous phase of data in Figure 3b. Phase changes dramatically (nearly 90°) at the edges of the prominent anomaly providing further strong evidence for sharp transitions (edges). e) Amplitude envelope for data in Figure 3a. Amplitude envelope provides a visual representation of reflection strength, and appears to be the most valuable single indicator of a potential tourmaline-bearing zone.

The velocity of the signal in air is 30 cm / ns, (GSSI, 1994). The initial estimate for velocity of the signal in the pegmatite was 10 cm / ns, based on a nominal dike dielectric value of 8 and previous experience in granitic pegmatites, (Patterson, 1996, Cook and Vasudevan, 1997). As the transmitting and receiving antennas are housed within the same shielded enclosure, a “zero offset section” was recorded directly. Traces were vertically stacked as they were recorded to increase the amplitude of anomalies and smooth the recorded information.

Our estimated maximum resolution and range of the 1,000 MHz antenna is about 2.5 cm at 1 m distance in granitic pegmatites (based on  $\frac{1}{4}$  of the signal wavelength of about 10 cm). Therefore, a nominal 75 cm range was established, for a two way travel time of 15 ns. The impulse signal was set at 1 ns at a rate of 32 pulses per second. Each 15 ns trace was sampled at discrete 8 bit, 512 spaced intervals with the following parameters: vertical high pass filter = 250 MHz, vertical low pass filter =

2000 MHz, horizontal smoothing = 4 scans, and a transmit rate = 64 KHz. The recording gains were set automatically at 5 points by recording a test signal during system setup prior to the scanning session when the antenna was held firmly against a relatively flat portion of the dike face, (GSSI, 1994). The traverse rate was established at approximately 20 cm per second. The most important operator condition of each scan was to traverse the surface at a constant rate, at nearly a constant separation from the dike, and to not halt the traverse or touch the rock face, which would cause a false return. Marker lines were added during the scan at pre-measured points on the dike, as well as at predetermined turn-around points. In this way, a monitored symmetry could be observed on each scanned section.

The recorded scan was played back immediately for preliminary interpretation. The only signal processing available at playback time was re-mapping of the amplitude of the signal to different color schemes and scales, (i.e., square root, logarithmic, power, etc.) as provided by the fixed operating system. We chose to image the scan using the variable density plot, with a linear color scale giving a black background with red positive and white negative amplitude images. A wiggle trace and single trace mode can also be displayed. We felt that the variable density image provided the optimum information in this underground mining situation.

After returning from the field, the data were transferred to a Compaq notebook computer. As the data were recorded in the GSSI \*.DZT format, files were read directly into the RADAN for Windows data processing software package for signal processing and manipulation. RADAN supports simple numerical calculations, trace editing, bandpass and FK filtering, Spiking Predictive Lag Deconvolution, Hyperbolic and Kirchoff Migration, and Complex Signal Trace analysis using the Hilbert Transform, (GSSI, 1995).

Because recording was accomplished in continuous mode between specified endpoints, rapid and complete coverage over a small area was possible, although at the expense of discretized, but more accurately known, position points. This approach was effective because the length of dike over which we measured the signal was long (two to tens of meters), and when anomalies were found, the continuous profiling provided very well defined anomaly signals. Furthermore, the narrow width of the dike (usually less than 1 meter) did not warrant advanced 3-D acquisition to identify and characterize the anomalies. In the mining environment, turnaround time for interpreted data necessarily needs to be short. If the practicality of the method could be demonstrated, mining time, production costs, and destroyed material could be reduced.

## Data Processing

Data processing of radar data can be similar to processing for seismic reflection data as the returned signal provides a time series for each trace. Because these data were recorded in continuous mode along a linear profile, we found that the most effective processes were those that assisted in characterizing anomalies according to frequency (Figure 3c), phase (Figure 3d) and amplitude (Figures 3e). A series of deconvolution and migration tests (not shown here) provided little improvement in the data, and in most cases degraded them; hence, the data were processed using complex trace analysis (Taner et al., 1979) that provides information about local variations in frequency, phase and amplitude and that can thus be valuable in tracking characteristics of anomalies. Instantaneous frequency of radar data, for example, assists in delineating variations in water content, dielectric values, or rock density.

Although the amplitude plots (Figure 3e) do not appear to provide much additional information over the raw scan of File 441 (Figure 3b), annotated plots of the amplitude envelopes of interpreted scans were provided to the blasting captain to aid in setting charges. We found that the miners had a much easier time assimilating the data from the amplitude plots than from the raw data plots. The amplitude envelopes appeared to be closer representations of their concept of the shape of a pocket formation.

## Discovery - The Cornucopia Pocket - File 441

File 441 was recorded in a part of the Himalaya dike that was no longer actively mined; here the dike exhibits few geological features that indicate pocket formation (Figure 3a). For example, there are no large schorl crystals fanning toward the center of the dike, no lepidolite pods, and the dike was mostly covered in dark green blast dust (Figure 3a). Accordingly, with no obvious mineralogical indicators, gem-bearing cavities could be easily missed.

The centerline of the GPR scan was located in the upper half of the 40 cm thick dike (Figure 3a) along a traverse of about 2.3 m length. Preliminary interpretations of the unprocessed scan (Figure 3b) identified two promising areas: a small set of anomalies (location indicated by paint in Figure 4a) at about 3-5 ns near 0.5 m on the radar scan (Figure 3b), and a more prominent anomaly at longer travel time (6.2-7.5 ns) centered near 1.5 m (Figure 3b).

Following each scan session, the recorded image was replayed for an initial cursory examination. File 441 exhibited several of the characteristics that could represent a pocket, including large amplitude variations over short distances in a hyperbolic shape. Variations in wall roughness and traverse rate can affect the shape of an anomaly, but in this case, the response appeared promising.

Comparison of the instantaneous frequency plot (Figure 3c) to the original scan (Figure 3b) indicates a rapid lateral change in frequency near 1.2 m, and thus a sharp transition on the left edge of the anomaly. In contrast, instantaneous phase calculations provide evidence of lateral phase shifts on the data (Figure 3d). When none is present, signals can be easily correlated laterally (Figure 3d). However, the edges of the anomalous region are delineated very well where the phase changes by nearly 90° near 1.2 m and near 1.8 m (Figure 3d).

A third characteristic provided in complex analysis, the amplitude envelope or reflection strength (Taner et al., 1979), has provided the most convincing evidence of a potentially productive zone of all of the processes that were investigated (Figure 3e). While the major anomaly exhibits recognizable characteristics on all of the figures, smaller, more subtle anomalies (e. g., near 0.5 m at 4 and 8 ns) are most visible by examining reflection strength (Figure 3e), and in some cases even these small anomalies have proven to be associated with cavities that contain gem crystals. Following complex trace analysis and careful evaluation, the location of File 441 was revisited for excavation (Figure 4).

The depth (distance into the rock mass) scale of the GPR reading is uncertain before excavation because the speed of the electromagnetic signals in the rock is unknown. Precise knowledge of the depth location of an anomaly is necessary, however, so that an explosive charge can be set to allow excavation of a pocket without destroying the contents. Distance can be estimated by the travel time of the signal and the velocity of the signal in the rocks if known. From our work in other pegmatites of the region and in crystalline rocks elsewhere (Patterson, 1996, Cook and Vasudevan, 1997), we

estimated the velocity at 0.10 m/ns. Thus, for a two-way travel time of 10 ns, the distance would be about 0.50 m. Accordingly, the anomaly in File 441 at about 6.2-7.5 ns was predicted to be about 0.31-0.37 m into the wall of the mine (Figure 4a).

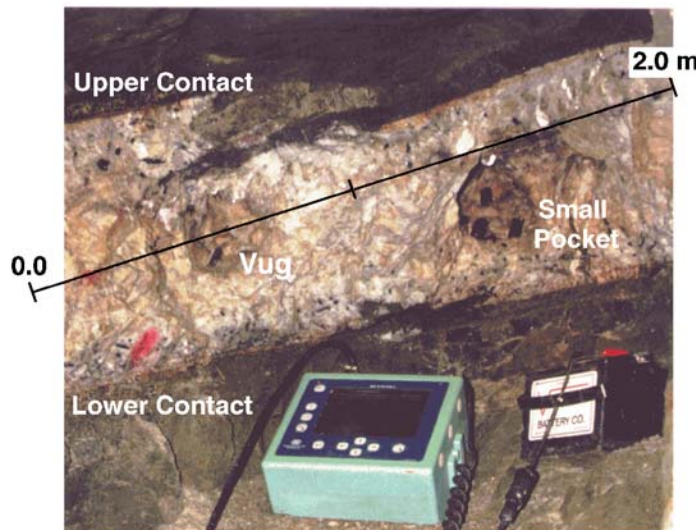
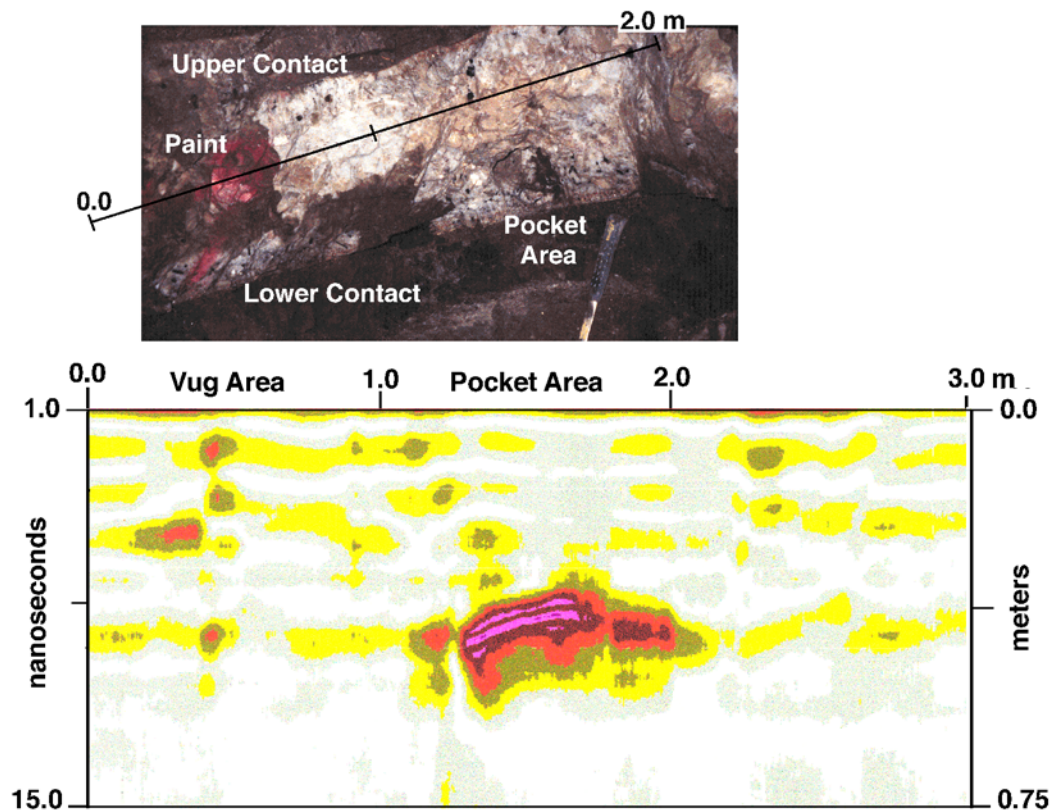




Figure 4. a) A section of dike in the region of the discovery pocket during excavation. Here the dike is about 45-50 cm thick, and there are few signs of pocket development. The line with 0.0-2.0 m marks is line of traverse along the dike made with the radar antennas; meter marks correspond to those on the scan in Figure 3e. Radar scan (1,000 MHz) after processing for amplitude envelope is shown in the lower part of the figure at the same scale to indicate the location of the major anomalies along the dike. Note high amplitude anomaly near 1.5 m at about 7-8 ns (about 0.35-0.40 m for a velocity of 0.1 m/ns). Anomalies near 0.5 m at about 3-5 ns (about 0.15-0.25 m) were interpreted as small vugs (Figure 4b). b) Excavated pocket and vug area with GSSI SIR-2 instruments in foreground. The distance marks are the same as those on radar scan in Figure 4a. Three tourmaline crystals that were excavated and then placed back in the cavity for the photograph are visible within the small pocket, and a single crystal is visible in one of the vugs. c) Enlargement of the discovery pocket with three large and two small tourmaline crystals placed back in the cavity for the photograph. Note triangular book of epitaxial lepidolite that hangs from ceiling; this mica is also visible in Figure 4a.

Following excavation, a pocket with a cornucopia shape was found at 0.32 m from a point normal to the face of the wall at location 1.5 m on the traverse. The pocket opening was about 0.12-0.15 m wide and faces downward to the right; the pocket projects about 0.42 m up to the left where it narrows to a point (Figures 4b and 4c). In the midsection, along the line of scan, the cavity widened to about 45cm as shown in Figures 6a and 6b. Its contents included 3 transparent, multicolored elbaite tourmaline crystals up to about 6 cm length x 3 cm diameter (Figure 5b), several bent and strained segments, and one doubly terminated flattened pink elbaite tourmaline crystal.

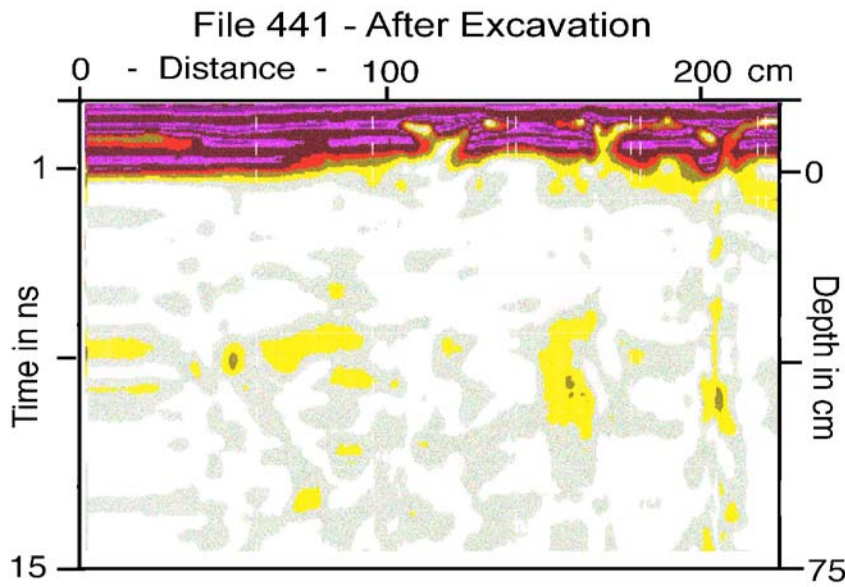


Figure 5. Radar scan (900 MHz) of the dike along the same line of profile as in Figure 4a after pocket 441 was excavated. Note that the scale is twice that of the previous scans, but that a small anomaly near 0.5 m at 8 ns is still visible and provides a visual correlation with the scan prior to excavation. However, the region of both the major anomaly (1.0-1.5 m) as well as the minor anomalies (0.5 m near 4 ns) is almost completely devoid of any returned signal. The major geological difference between this scan and the scan in Figures 3 and 4 is that the face of the pocket and the tourmaline crystals have been removed from the cavities, it appears as though the prominent anomalies were due to the presence of crystals, rather than to the air filled cavities.

The pocket was an air filled void, with minor microcline feldspar and quartz along the walls, that extended almost from contact-to-contact along the rake of the dike (Figures 6a and 6b). This contrasts with the many red clay or zeolite filled flattened pockets that tend to be localized in the center or upper 1/3 of the dike and that have previously been assumed to be "typical" in these kinds of dikes (Foord, 1976, Figure 2b). The implication of this discovery is that there may be many pockets that do not fit either with assumed indicators or with the expected geometry. In addition to the "cornucopia pocket", several small vugs were encountered during excavation of this portion of dike that were visible on the GPR scan and were predicted from initial interpretations, (paint area in Figure 4a). For example, two vugs each contained a single multicolored elbaite crystal (Figure 4b). Additionally, the walls of pocket 441 were relatively smooth, thus minimizing signal scattering.

Following the excavation of the pocket and vugs at the location of File 441, the dike was re-scanned with a 900 MHz central frequency antenna (Figures 5 and 6b) as the 1000Mhz antenna was not available when the re-scan was done. Nevertheless, this provided a comparison with the scan before excavation. The post-excavation scan (Figure 5) provides little or no evidence of anomaly near 1.5-2.0 m, even though part the cavity is still present and even somewhat enlarged from the excavation. Similarly, the vug that contained a single tourmaline crystal near 0.5 m at 4 ns is also no longer visible,

whereas a small anomaly near 7-8 ns at about 0.5 m is still present. The differences between Figures 5 and 3e are most likely due to the opening of the cavities and removal of their contents. Since approximately 30 cm of dyke was removed (Figure 6), the GPR signal would be included in the first ns of the pulse. The airwave is apparent, with small aberrations where only 10-30 cm were removed between the pocket at 1.5 m and the vug at 0.5 m (Figures 6d).

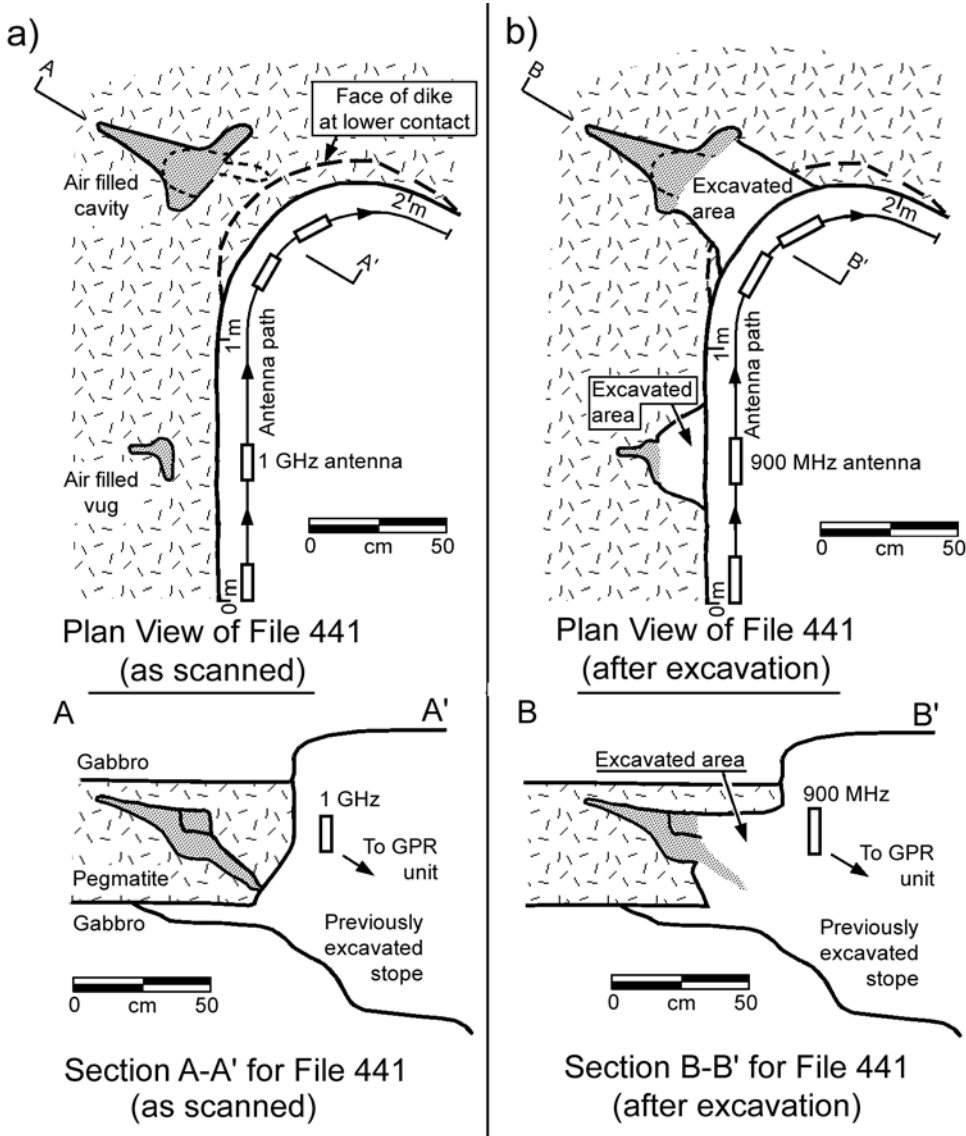


Figure 6. Drawing of the File 441 pocket area before (a) and after (b) excavation. Both plan views (upper) and cross-sectional views (lower) are illustrated to provide information on the shape of the pocket and vug that were excavated. Pocket area is shown by dotted pattern.

The scanned image from File 441 presented a pristine example of an anomaly found in over 500 scanned areas. This allowed us to clearly delineate the features that would be useful for rapid analysis of less pristine and noisier data. Comparison of the original scan (Figure 3a) with the modeling of Goodman, (1994), and Götsche, (1997), provides evidence that File 441 is an air, rather than red clay, filled pocket. For example, because the impulse is 1 ns in length and the wavelength ( $\lambda$ )

in air is 30cm, there appear to be two major reflections, interpreted to be from the front and back wall of the pocket, with later multiple reflections. Based on the excavated distances between the pocket walls of 15 cm, the reflection from the back of the pocket would arrive ~1 ns after the reflection from the front of the pocket. The smooth walls of this pocket probably contributed to the pristine nature of the returned signal. In contrast, Figures 7a and 7b illustrate signals from pockets filled with red clay (Figure 7a), and another air filled pocket (Figure 7b), both of which contained gem tourmaline (Table 1). The similarity of these two responses implies that it may often be difficult to distinguish between clay filling and air filling from the GPR signal alone. The contribution of the piezo-electric gem tourmalines to the strong amplitudes, if any, remains to be studied.

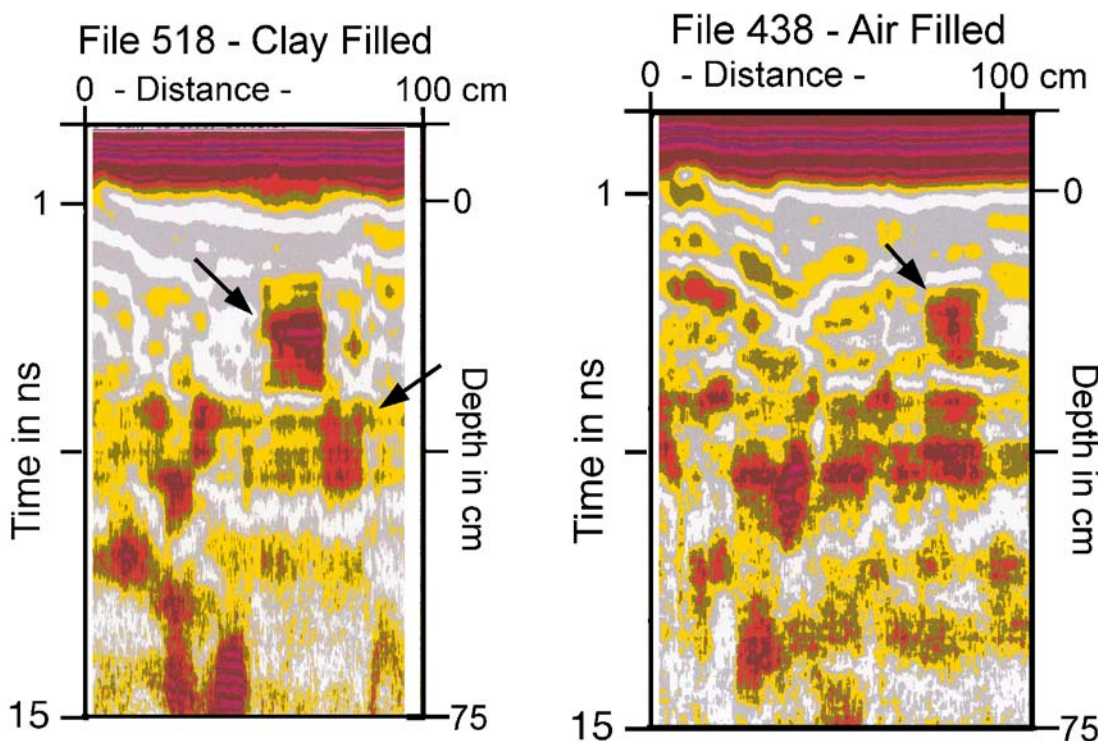


Figure 7. a) GPR response from file 518 that includes anomalies from two pockets filled with red clay. Both of these pockets contained elbaite tourmaline (Table 1). b) GPR response from File 438 that includes an image of an air-filled pocket (arrow) that was similar to, but slightly smaller than, the pocket at 441. Note that the response is not as clearly hyperbolic, nor are there obvious multiple reflections. The pocket was excavated and contained crystals of quartz, potassium feldspar, and green elbaite tourmaline (Table 1). The later anomalies have not been excavated. Note the similarity of the responses to that in (a).

Once the discovery of the cornucopia pocket at File 441 was established, all the previous and subsequent results that we had acquired in this mine could be calibrated for the nature of the signal, the signal velocity and the processing parameters. For the next seven weeks, more than 1,000 lineal meters of dyke were surveyed, scanned, interpreted, and selected areas excavated. The calibrated signal allowed identification and excavation of seven (7) additional pockets (one of which is shown in Figure 2b) and twenty five (25) additional vugs which contained gem elbaite tourmaline, other rare minerals such as morganite beryl, hambergite, and bavenite, and more typical microcline, cleavelandite, and quartz. The contents and attributes of these features are listed in Table 1.

## Conclusions

The development of high resolution geophysical methods, particularly ground penetrating radar, to produce detailed images of subsurface structures has led to the ability to identify gem tourmaline-bearing zones within the Himalaya sheeted pegmatite in southern California. When appropriately recorded, processed and calibrated with geological information, resolution of features (pockets and vugs) as small as a few cm within approximately 2 m, or 10's of cm within about 5 m of a wall surface may be obtained. This approach thus provides an opportunity to find gem-bearing zones that may not exhibit "typical" indicators and/or that may be in areas that are no longer actively mined.

## Acknowledgments

Supported by Canadian Natural Sciences and Engineering Research Council. We thank the mine owners for allowing us access to the Southern California pegmatites reported in this study: Himalaya Mine, Pala International, Inc., William F. Larson, Sr., President, John McLean, Mine Manager, and Benjamin Castillo, Blasting Captain; Little 3 Mine, Louis B. Spaulding, Jr.; Tourmaline Queen Mine, Mr. Edward Swoboda. Kris Vasudevan provided helpful discussions and assistance in data processing, Bob Scarborough assisted with organization and fieldwork, Jim Means, Jeff Krogstad, and Mike Menzies provided capable assistance in the field work. We owe a particular debt to the late Eugene E. Foord, USGS, for his many helpful discussions.

## REFERENCES

- Arcone, S.A., Lawson, D.E., Delaney, A.J., Strasser, J.C., and Strasser, J.D., 1998, Ground-penetrating radar reflection profiling of groundwater and bedrock in an area of discontinuous permafrost, *Geophysics*, **63**, p. 1573-1584.
- Bitri, A., and Grandjean, G., 1998, Frequency-wavenumber modeling and migration of 2D GPR data in moderately heterogeneous dispersive media, *Geophysical Prospecting*, **46**, p. 287-301.
- Conyers, L.B. and Goodman, D., 1997, *Ground-Penetrating Radar, An Introduction for Archaeologists*, AltaMira Press, Walnut Creek, California, pp. 232.
- Cook, F.A., 1997, Applications of geophysics in gemstone exploration, *Gems and Gemology*, **33**, p. 4-23.
- Cook, F.A. and Vasudevan, K., 1997, Georadar anisotropy in the Gotthard gneiss, Switzerland, *Geophysical Research Letters*, **24**, p. 197-200.
- Cook, J.C., 1973, Radar Exploration Through Rock in Advance of Mining, *Transactions of the Society of Mining Engineers of AIME*, **254**, 140-146.
- Cook, J.C., 1975, Radar transparencies of mine and tunnel rocks, *Geophysics*, **40**, 865-885.
- Daniels, J.J., 1988, Locating caves, tunnels and mines, *The Leading Edge*, **7**, p. 32-37,52.
- Dolphin, L.T., Beatty, W.B., and Tanzi, J.D., 1978, Radar probing of Victorio Peak, New Mexico, *Geophysics*, **43**, p. 1441-1448.
- Donnelly, M. G., 1935, The lithia pegmatites of Pala and Mesa Grande, San Diego County, California, Unpublished Ph.D. thesis, California Institute of Technology, Pasadena, California, 117 pp.
- Fisher, J., Foord, E. E., and Bricker, G. A. 1998. The geology, mineralogy, and history of the Himalaya mine, Mesa Grande, San Diego County, California, *Rocks & Minerals*, **73**, p. 156-180.
- Foord, E. E., 1976, Mineralogy and petrogenesis of layered pegmatite-aplite dikes in the Mesa Grande district, San Diego county, California, Unpublished Ph.D. thesis, Stanford University, Stanford, California, 326 pp.
- Foord, E.E., 1977, The Himalaya Dike System, Mesa Grande District, San Diego County, California, *Mineralogical*

Record, **8**, p. 461-474.

Franké, J.C. and Nobes, D.C., 2000, *A preliminary Evaluation of GPR for Nickel Laterite Exploration*, in Noon, D.A., Stickley, G.F., and Longstaff, D., eds., GPR 2000 Proceedings of the Eighth International Conference on Ground Penetrating Radar, SPIE 4084, p. 7-12.

Geophysical Survey Systems Inc., 1994, SIR - II Operation Manual, Geophysical Survey Systems, Inc., North Salem, New Hampshire, Manual #MN72-140.

Geophysical Survey Systems Inc., 1995, RADAN for Windows, Beta Version 1.4, Geophysical Survey Systems, Inc., North Salem, New Hampshire, Manual #MN43-116.

Geophysical Survey Systems Inc., 2001, Mining, Geophysical Survey Systems, Inc., North Salem, New Hampshire, <http://www.geophysical.com.mining.htm>.

Glover, J.M., 1992, Void detection using standing wave analysis, in Pilon, J., ed., Ground penetrating radar, Geological Survey of Canada Special Paper 90-4, p. 63-73.

Goodman, D., 1994, Ground-penetrating radar simulation in engineering and archaeology, *Geophysics*, **59**, p. 224-232.

Göttsche, F.-M., 1997, Identification of Cavities by Extraction of Characteristic Parameters from Ground Probing Radar Reflection Data, Unpublished Ph.D. Thesis, Christian-Albrechts Universität, Kiel, Germany, 122 pp.

Grasmueck, M., 1996, 3-D ground-penetrating radar applied to fracture imaging in gneiss, *Geophysics*, **61**, p. 1050-1064.

Holloway, A.L., 1992, Fracture mapping in granite rock using ground probing radar, in Pilon, J., ed., Ground Penetrating Radar, Geological Survey of Canada, Paper 90-4, p. 85-100.

Krummenacher, D., Gastil, R. G., Bushee, J., and Doumont, J., 1975, K-Ar apparent ages, Peninsular Ranges batholith, Southern California and Baja California, *Bull. Geol. Soc. America*, **86**, p. 760-768.

Lees, B.K., 1998, The Application of Ground-Penetrating Radar to Mineral Specimen Mining, *Mineralogical Record*, **29**, p. 145-153.

Noon, D.A., Stickley, G.F., and Longstaff, D., eds., 2000, GPR 2000 Proceedings of the Eighth International Conference on Ground Penetrating Radar, SPIE 4084, pp. 908.

Olhoeft, G.R., Powers, M.H., and Capron, D.E., 1994, Buried Object Detection with Ground Penetrating Radar, in Proceedings of Unexploded Ordnance (UXO) detection and range remediation conference, Golden, CO, May 17-19, 1994, 207-233.

Olsson, O.L., Falk, O., Forslund, O., Lundmark, L., and Sandberg, E., 1992, Borehole radar applied to the characterization of hydraulically conductive fracture zones in crystalline rock, *Geophysical Prospecting*, **40**, 109-142.

Patterson, J. E., 1996, Modeling miarolitic cavities in a pegmatite dike using subsurface interface radar, Little Three Mine, Ramona, California, in *The Spirit of Inquiry*, undergraduate research sponsored by the Honors Center, University of Arizona, Tucson, p. 17.

Patterson, J. E., and Cook, F. A., 1999, Successful application of Ground penetrating radar in exploration for gem tourmaline (abstract), *Canadian Mineralogist*, **37**, p. 862-863.

Patterson, J.E., and Cook, F.A., 2000, *Application of Complex Trace Analysis for Improved Target Identification in Gem Tourmaline Bearing Pegmatites, Himalaya Mine, San Diego County, California*, in Noon, D.A., Stickley, G.F., and Longstaff, D., eds., GPR 2000 Proceedings of the Eighth International Conference on Ground Penetrating Radar, SPIE 4084, 653-657.

Pilon, J.A., ed., 1992, Ground Penetrating Radar, Geological Survey of Canada, Paper 90-4, pp. 241.

Silver, L.T., Taylor, H.P. and Chappell, B., 1979, Some petrological, geochemical, and geochronological observations of the Peninsular Ranges batholith near the international border of the U.S.A. and Mexico, in Abbott, P.L., and Todd, V.R., eds., Mesozoic crystalline rocks: Peninsular Ranges batholith and Pegmatites, Sal Point Ophiolite, San Diego, California, San Diego State University, Department of Geological Sciences, p. 83-110.

Taner, M. T., Koehler, F., and Sheriff, R. E., 1979, Complex seismic trace analysis, *Geophysics*, **44**, p. 1041-1063.

Trickett, J.C., Stevenson, F., Vogt, D., Mason, I., Hargreaves, J., Eybers, H, Fynn, R., and Meyering, M., 2000, The

- Application of Borehole Radar to South Africa's Ultra-Deep Gold Mining Environment, in Noon, D.A., Stickley, G.F., and Longstaff, D., eds., GPR 2000 Proceedings of the Eighth International Conference on Ground Penetrating Radar, SPIE 4084, p. 676-681.
- Ulrickson, C.P., 1982, Application of Impulse Radar to Civil Engineering, Ph.D. Thesis, Lund University of Technology, Lund, Sweden, 175 pp.
- Wensink, W.A., Greeuw, G., Hofman, J., and Van Deen, J.K., 1990, Measured underwater near-field E-patterns of a pulsed, horizontal dipole antenna in air: comparison with the theory of the continuous wave infinitesimal electric dipole, Geophysical Prospecting, **38**, p. 805-830.
- Zeng, X., and McMechan, G.A., 1997, GPR characterization of buried tanks and pipes, Geophysics, **62**, p. 797-806.